

## Calcium Efflux as a Component of the Hypersensitive Response of *Nicotiana benthamiana* to *Pseudomonas syringae*

Lev G. Nemchinov<sup>1,\*</sup>, Lana Shabala<sup>2</sup> and Sergey Shabala<sup>2,\*</sup>

<sup>1</sup> USDA/ARS, Plant Sciences Institute, Molecular Plant Pathology Laboratory, Beltsville, MD 20705, USA

<sup>2</sup> School of Agricultural Science, University of Tasmania, Private Bag 54, Hobart, Tasmania 7001, Australia

Using a model plant *Nicotiana benthamiana*, we have demonstrated that initial calcium uptake in response to the HR (hypersensitive response)-causing pathogen *Pseudomonas syringae* pv *syringae* 61 is followed by net calcium efflux initiated at about 12 h after the bacterial challenge and sustained for at least 48 h. Our data suggest that calcium not only acts as an important second messenger in the activation of resistance responses but may also be a downstream mediator of later cell death acceleration and completion of the defense reaction. Accordingly, we propose that the existing model of HR should be amended to include a PM  $\text{Ca}^{2+}$  ATP pump as an important component of the HR to pathogens in plants.

**Keywords:** Calcium efflux — Hypersensitive response — *Pseudomonas syringae*.

Abbreviations: Avr, avirulence factor; CPA, cyclopiazonic acid; HR, hypersensitive response; MIFE, microelectrode ion flux estimation; PAMP, pathogen-associated molecular pattern; PM, plasma membrane.

### Introduction

Innate immunity in plants is an interdependent combination of two different recognition pathways—two consecutive security barriers on a pathogen's way to successful infection. The first mechanism is a broad, non-specific interaction of the microbe with a plant cell, and it relies on highly conserved pathogen-derived signals or structural characteristics, so-called pathogen-associated molecular patterns, PAMPs (Jones and Dangle 2006). PAMP-based recognition is thought to be a key event in non-host resistance, i.e. incompatibility of the majority of host–pathogen combinations. The second defense mechanism, gene-for-gene interactions (Flor 1971), is activated by specific recognition of a pathogen's avirulence factors (Avr) by host resistance genes (*R* gene), and results in disease resistance frequently in the form of hypersensitive cell death (HR). It was recently proposed that these two pathways complement each other successively in a zigzag fashion (Jones and Dangle 2006).

It is widely acknowledged that ion fluxes across cellular membranes play a key role in triggering and mediating defense mechanisms (Grant et al. 2000, Lam et al. 2001, Gomez-Gomez and Boller 2002, Pike et al. 2005). Plant ion channels are rapidly modulated in response to environmental stimuli and ion fluxes appear to be one of the earlier events in pathogen recognition.

Calcium acts as an important second messenger, which passes on and amplifies signals received at receptors on the cell surface—including signals from pathogens—to target molecules in the cytosol and activate resistance responses, in particular the HR (Atkinson et al. 1990, Levine et al. 1996, Jabs et al. 1997, Grant et al. 2000, Heath 2000, Lam et al. 2001, Balagué et al. 2003, Pike et al. 2005, Lecourieux et al. 2006, Hann and Rathjen 2007). Calcium channel blockers were shown to inhibit the HR in tobacco and soybean systems (Atkinson et al. 1990, Levine et al. 1996). It was suggested that calcium influx is required for HR initiation and that HR, once initiated, requires sustained  $\text{Ca}^{2+}$  influx (Atkinson et al. 1990).

A Gram-negative, plant-pathogenic bacterium *Pseudomonas syringae* is a model organism in plant pathology. *Pseudomonas syringae* strains are noted for their diverse and host-specific interactions with different plant species. It has been previously demonstrated that inoculation of host plants with the bacterium *P. syringae* causes influx of calcium ions, which is an essential component in signal transduction pathways leading to the oxidative burst, defense responses and activation of the HR (Levine et al. 1996, Grant et al. 2000, Balagué et al. 2003). A biphasic increase in cytosolic calcium influx was detected in *Arabidopsis* plants challenged by *P. syringae* pv *tomato*: an initial calcium increase was elicited in an *R*-gene-independent manner followed by a second burst, which required a functional RPM1 (*R*-gene protein) gene product (Grant et al. 2000). Thus, an important role for calcium signaling in induction of defense responses, both broad, PAMP-associated and specific gene-for-gene interactions characteristic for the HR, is undisputed.

In this work, we studied ion fluxes generated on a model plant *Nicotiana benthamiana* in response to a challenge with the HR-causing pathogen, incompatible

\*Corresponding authors: Lev Nemchinov, E-mail, Lev.Nemchinov@ars.usda.gov; Fax, +1-301-504-5449; Sergey Shabala, E-mail, Sergey.Shabala@utas.edu.au; Fax, +61-3-6226-2642.

*P. syringae* pv *syringae* 61. Elicitation of the HR by *P. syringae* pv *syringae* 61 on tobacco plants was previously reported (Huang et al. 1988). We have demonstrated that initial calcium uptake characteristic of *P. syringae* infection, and as described elsewhere (Grant et al. 2000, Pike et al. 2005, Hann and Rathjen 2007), is followed by the well-defined calcium efflux initiated 12–48 h after the challenge. We are not aware of any reported observations to date suggesting efflux of  $\text{Ca}^{2+}$  as part of the *P. syringae*-induced HR process. We suggest that this pattern of calcium signaling may indicate that *P. syringae*-induced HR is a multistep process and consists of several phases. An initial calcium entry into the cells is required for the induction of the basal defense response and activation of the HR, while the late calcium efflux could potentially reflect its functional role in the development of a more expanded cell death. This assumption is in accordance with a general role for calcium homeostasis in plants (Gilroy et al. 1993).

## Results

### *Pseudomonas syringae* pv *syringae* 61 causes typical HR in *Nicotiana benthamiana*

Characteristic HR symptoms (necrotic rings and spots at the site of infiltration) were evident on plants inoculated with *P. syringae* pv *syringae* 61 within 24–30 h after the challenge. Necrotic lesions did not spread beyond the initial infiltration area during the 1 month observation period after inoculation (Fig. 1A). In contrast, *N. benthamiana* plants were susceptible to the virulent pathogen *P. syringae* pv *tabaci* which caused spreading necrosis, severe chlorosis of the leaf lamina, yellowing and tissue collapse 72 h after the challenge (Fig. 1A). These data are consistent with previously reported experiments (Huang et al. 1988).

### $\text{Ca}^{2+}$ flux signaling is associated with early stages of bacterial treatment

Addition of bacterial inoculum to the measuring chamber caused a rapid and transient elevation in net  $\text{Ca}^{2+}$  uptake by leaf mesophyll (Fig. 1B). The rapidity of the response (peaking ~1 min after treatment) may suggest either direct association of  $\text{Ca}^{2+}$ -permeable channels with plasma membrane (PM) PAMP recognition receptors or a very short signaling pathway from the receptors to the channels. This initial 'receptor-type'  $\text{Ca}^{2+}$  uptake was short-lived and disappeared within 6–10 min after the challenge (Fig. 1B).

It is known that mesophyll cells respond to light fluctuations by significant changes in PM potentials (Elzenga et al. 1995). Onset of illumination causes a transient membrane depolarization (peaking 2–3 min after the light treatment) and light-induced  $\text{Ca}^{2+}$  uptake. Onset of illumination (bright light  $2,500 \mu\text{mol s}^{-1} \text{m}^{-2}$ ) caused a significant increase in net  $\text{Ca}^{2+}$  uptake in *N. benthamiana* mesophyll

cells (Fig. 1C), from  $4.6 \pm 0.6 \text{ nmol m}^{-2} \text{ s}^{-1}$  in the dark to  $19.5 \pm 2.1 \text{ nmol m}^{-2} \text{ s}^{-1}$  in the light. Leaves treated with bacteria for 1 h showed a very similar magnitude of response (light flux level  $22.3 \pm 3.6 \text{ nmol m}^{-2} \text{ s}^{-1}$ ). However, there was a clear trend of increasing the magnitude of  $\text{Ca}^{2+}$  uptake in light as the time of incubation with bacteria increases (Fig. 1C). In contrast, in control samples (Fig. 1D), no apparent tendency was observed. Based on these data we suggest that the time interval between 10 and 60 min after the challenge (when the  $\text{Ca}^{2+}$  response to bacteria is 'silent') reflects the transition period from the basal PAMP-triggered response to the sustained *R*-gene-dependent calcium increase, similar to what was proposed by Grant et al. (2000). Then a gradual increase in net  $\text{Ca}^{2+}$  uptake is triggered (Fig. 1C). As soon as 2 h after *P. syringae* treatment, net  $\text{Ca}^{2+}$  uptake both in light and in the dark was about 2-fold higher compared with control (significant at  $P < 0.05$ ; Fig. 1C). Even higher  $\text{Ca}^{2+}$  uptake values were measured after 3 h treatment (Fig. 2).

### Long-term bacterial exposure results in net $\text{Ca}^{2+}$ efflux

Increased  $\text{Ca}^{2+}$  uptake associated with early events of bacterial pathogenesis on *N. benthamiana* and previously reported by many authors was observed only within the first several hours. The peak uptake occurred somewhere between 3 and 7 h after inoculation (Fig. 2A) and then started to decline. At 7 h after the challenge  $\text{Ca}^{2+}$  uptake was significantly ( $P < 0.05$ ) attenuated, both in the light and in the dark, compared with non-inoculated control (zero treatment). Twenty-four and 48 h later, net  $\text{Ca}^{2+}$  flux became substantially and progressively negative (Fig. 2B), implying active  $\text{Ca}^{2+}$  extrusion against the electrochemical gradient. Five days after challenge, leaf samples showed near zero net  $\text{Ca}^{2+}$  flux and lost their ability to respond to light/dark fluctuations (data not shown).

### Pharmacology of $\text{Ca}^{2+}$ flux responses

To provide insight into the role of specific membrane transporters mediating the observed  $\text{Ca}^{2+}$  flux responses, a series of pharmacological experiments was undertaken. Leaf segments inoculated with *P. syringae* pv *syringae* 61 for 3 h were incubated in a range of known  $\text{Ca}^{2+}$ -permeable channel blockers; the latter were applied 1 h prior to measurements. Both  $\text{Gd}^{3+}$  and  $\text{La}^{3+}$  significantly shifted dark  $\text{Ca}^{2+}$  flux values to net efflux (Fig. 3A). Moreover, onset of illumination led to a further increase in  $\text{Ca}^{2+}$  efflux from mesophyll cells (Fig. 3A). Pre-treatment with 1 mM  $\text{Cs}^+$  significantly ( $P < 0.05$ ) attenuated light-induced  $\text{Ca}^{2+}$  flux kinetics, but did not result in net  $\text{Ca}^{2+}$  efflux (Fig. 3A). In contrast, pre-treatment with cyclopiazonic acid (CPA; a known inhibitor of  $\text{Ca}^{2+}$ -ATPase) for 1–2 h significantly ( $P < 0.05$ ) increased net  $\text{Ca}^{2+}$  uptake both in the dark and in the light (Fig. 3B).

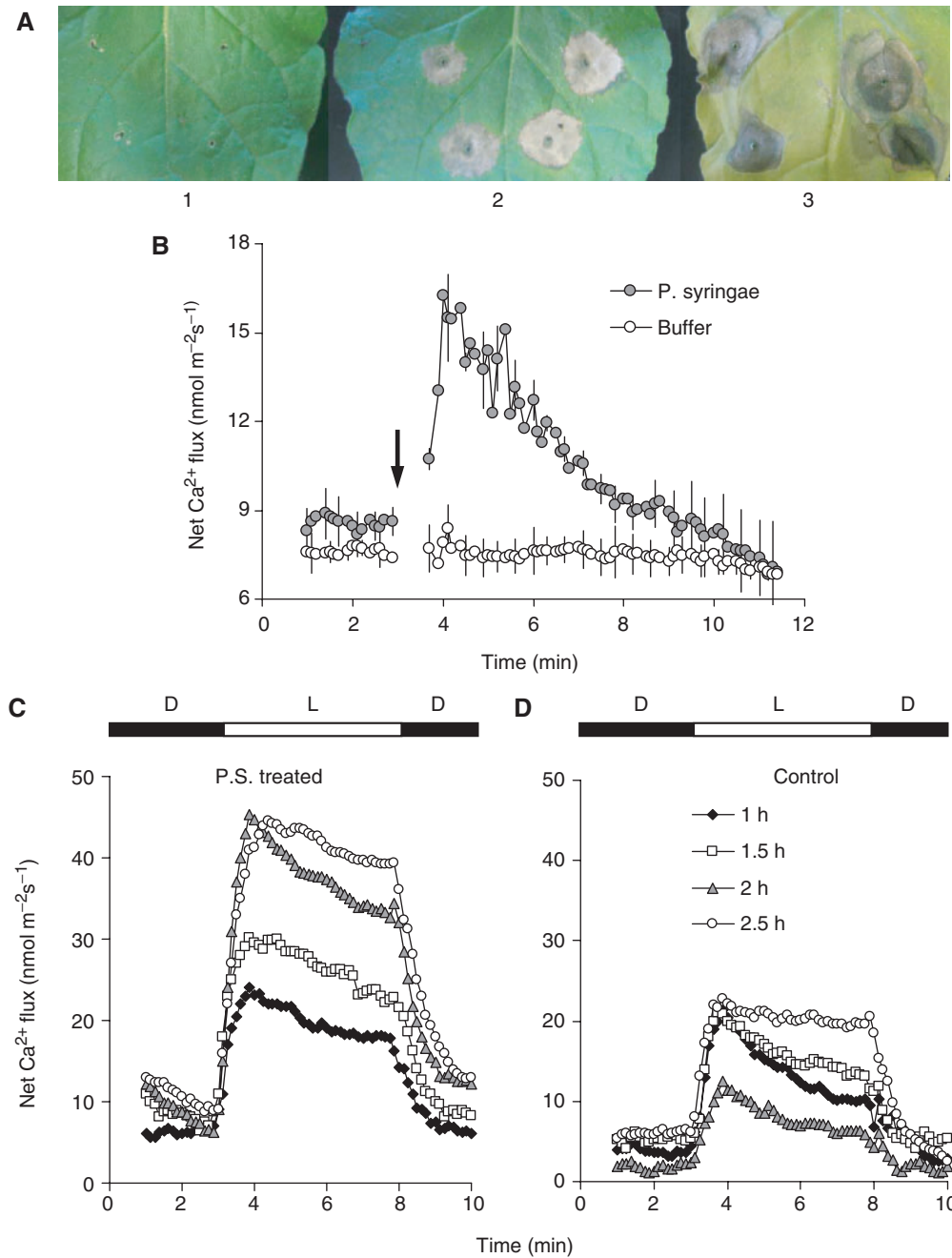


**Fig. 1** (A) Hypersensitive response (HR) on leaves of *Nicotiana benthamiana* plants inoculated with *Pseudomonas syringae* pv *syringae* 61. 1, Mock-inoculated plants; 2, plants inoculated with *P. syringae* pv *syringae* 61; 3, plants inoculated with the virulent strain *P. syringae* *tabaci*. Pictures were taken 1 week after inoculation. (B) Transient  $\text{Ca}^{2+}$  flux responses of *N. benthamiana* mesophyll cells to the treatment with *P. syringae* pv *syringae* 61. Filled symbols: bacterial stock (final OD = 0.25 after mixing with a bath solution) was added at 3 min as indicated by an arrow. Open symbols: 1 ml of the buffer solution added instead of *P. syringae* stock. Mean  $\pm$  SE ( $n = 4$  and  $3$ , respectively). For all MIFE data, the sign convention is 'influx positive'. (C) Kinetics of light (L)–dark (D) transient net  $\text{Ca}^{2+}$  flux responses of *N. benthamiana* mesophyll cells treated with bacteria for various times, between 1 and 2.5 h. (D) Control leaf segments incubated with buffer solution. Four individual traces are shown for each treatment. Measurements were started at dim microscope light ( $20 \mu\text{mol s}^{-1} \text{m}^{-2}$ ), and were then exposed to bright white light ( $2,500 \mu\text{mol s}^{-1} \text{m}^{-2}$ ) between 3 and 8 min. Note that the same symbols are applicable to C and D.

## Discussion

Most of preceding reports on this subject emphasize the role of calcium influx elevation in HR induction (Atkinson et al. 1990, Levine et al. 1996, Jabs et al. 1997, Grant et al. 2000, Lam et al. 2001, Balagué et al. 2003, Pike et al. 2005, Hann and Rathjen 2007). While our experiments confirmed these findings, we also found that after inoculation of *N. benthamiana* with the incompatible bacterium *P. syringae* pv *syringae* 61,  $\text{Ca}^{2+}$  influx occurs only at the first stages of pathogen–host interaction, during 0–7 h after the challenge. More importantly, we found that initial calcium uptake is subsequently followed by the net calcium efflux initiated between 10 and 12 h and continued up to 48 h after the challenge (Fig. 2). As passive  $\text{Ca}^{2+}$  efflux from the cell cytosol is thermodynamically impossible, the only two possible sources for it may be either  $\text{Ca}^{2+}$  release from the cell wall as a result of the Donnan exchange (Shabala and Newman 2000), or active  $\text{Ca}^{2+}$  extrusion via PM  $\text{Ca}^{2+}$ -ATPase. Our pharmacological

experiments (Fig. 3) completely rule out the first possibility and suggest that indeed such an efflux is mediated by a PM  $\text{Ca}^{2+}$ -ATP pump. Moreover, when net  $\text{K}^{+}$  fluxes were measured alongside  $\text{Ca}^{2+}$  at these times, no significant ( $P < 0.05$ ) difference between the magnitude of net  $\text{K}^{+}$  flux of control and *Pseudomonas*-treated samples was found (Table 1). These results provide additional support for the idea of  $\text{Ca}^{2+}$  efflux being a component of the HR response mechanism rather than a product of non-specific ion leakage through the PM. Whether it is causal of HR or accompanies it is a subject for further investigation. It is thus our opinion that these observations make an important contribution to understanding the timing, execution and mechanisms of defense signaling, and raise the possibilities of a distinct multiphase structure of the HR pathway.

The lack of such observations in previous studies is most probably explained by the range of experimental techniques used to study  $\text{Ca}^{2+}$  signaling during

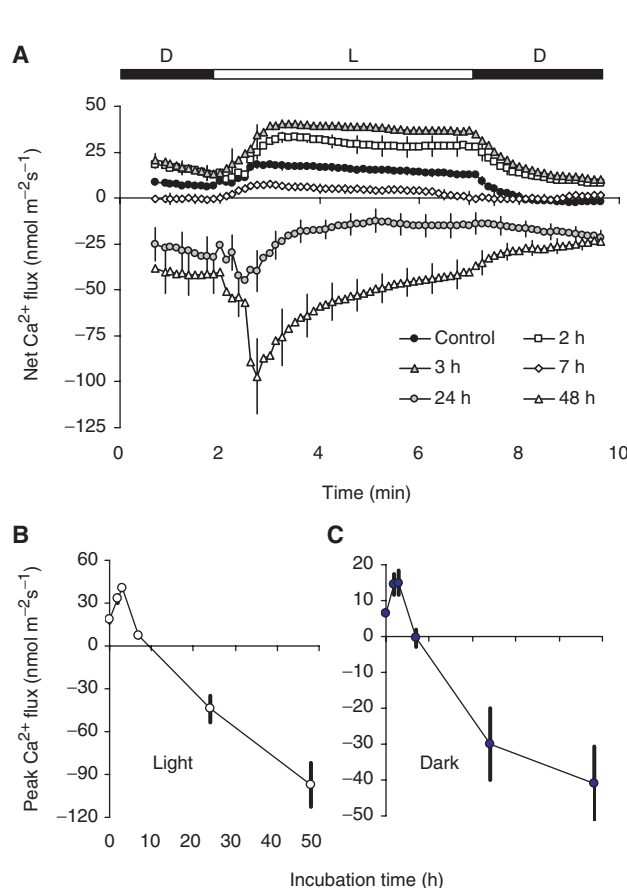


**Fig. 2** Time dependence of the effect of bacterial treatment on  $\text{Ca}^{2+}$  fluxes from tobacco mesophyll cells. (A) Transient light–dark net  $\text{Ca}^{2+}$  flux kinetics after various incubation times in *P. syringae* pv *syringae* 61 solution. (B and C) Peak  $\text{Ca}^{2+}$  flux in the light and in the dark, respectively. Mean  $\pm$  SE ( $n = 4–8$ ).

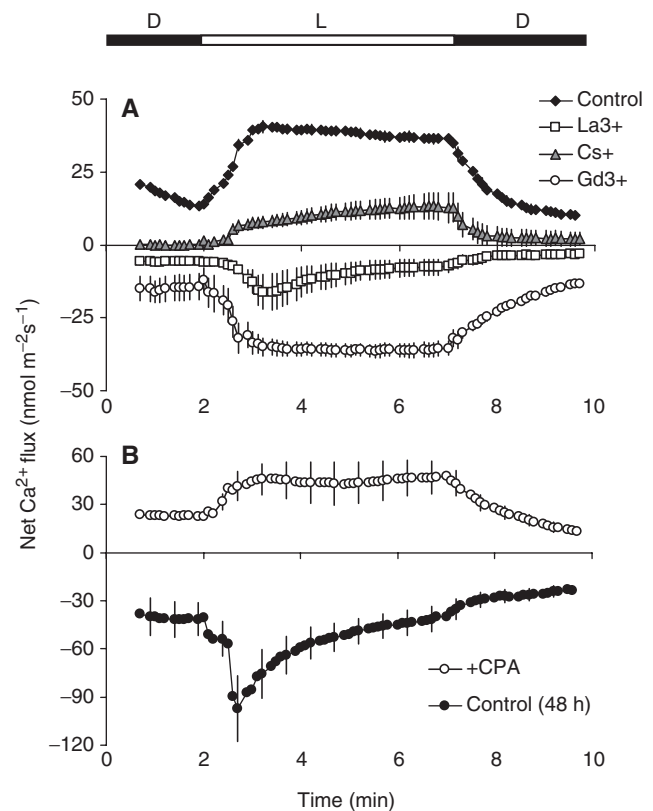


**Fig. 3** Pharmacology of  $\text{Ca}^{2+}$  flux responses. Mean  $\pm$  SE ( $n = 4–5$ ). (A) Leaf segments were treated with *P. syringae* pv *syringae* 61 (as described in Materials and Methods for short-term bacterial treatments) for 3 h prior to incubation for 1 h in an appropriate inhibitor. Concentrations used were as follows:  $\text{La}^{3+}$ , 1 mM;  $\text{Gd}^{3+}$  50 mM;  $\text{Cs}^{+}$ , 1 mM. (B) Light-induced net  $\text{Ca}^{2+}$  flux kinetics after 48 h of treatment with *P. syringae* pv *syringae* 61 in control (filled symbols) and after 2 h pre-treatment in 50  $\mu\text{M}$  CPA.

plant–pathogen interaction. The most common is the use of  $^{45}\text{Ca}^{2+}$  radiotracers (Atkinson et al. 1990). This method is measuring the unidirectional  $\text{Ca}^{2+}$  uptake only with low temporal resolution and, thus, is not capable either of resolving HR-associated  $\text{Ca}^{2+}$  efflux or providing an adequate resolution of the fast kinetics associated with early signaling events. Pharmacological evidence obtained by using lanthanides ( $\text{La}^{3+}$  and  $\text{Gd}^{3+}$ ) to block  $\text{Ca}^{2+}$  influx (Atkinson et al. 1990) also cannot be interpreted unambiguously as, being used at millimolar external concentrations, these lanthanides may enter the cell, thus affecting the PM  $\text{Ca}^{2+}$ -ATPase (Quiquampoix et al. 1990). As for the use of fluorescent dyes (Hann and Rathjen 2007), these cannot distinguish between transient  $[\text{Ca}^{2+}]_{\text{cyt}}$  changes occurring as a result of increased  $\text{Ca}^{2+}$  uptake from the external medium (e.g. PM mediated) and changes resulting from  $\text{Ca}^{2+}$  release from an internal store (such as a vacuole or the endoplasmic reticulum). The microelectrode ion flux estimation (MIFE)

technique appears to be free of these hurdles, allowing simultaneous determination of the ‘instantaneous’ net fluxes associated with a localized region of plant tissue (Shabala et al. 2006) and providing a convenient tool to study mechanisms involved in host–pathogen interactions and activation of the plant defense system.

Light-induced  $\text{Ca}^{2+}$  influx is usually associated with two physiological processes: (i) leaf expansion growth (in epidermal cells); and (ii) performance of PSII in mesophyll cells (Elzenga et al. 1995, Van Volkenburgh 1999, Zivanovic et al. 2007). Our findings that 5 d after *Pseudomonas* challenge leaf mesophyll samples lost their ability to respond to light/dark fluctuations may be indicative of the pathogen damage to PSII.

Based on our data, the following scenario may be considered:

1. The initial transient  $\text{Ca}^{2+}$  influx across the PM (first 1–10 min) is a result of interactions between PAMPs and host receptors, as described elsewhere (Grant et al. 2000). During this phase the plant performs an initial recognition of the invasive organism and activates basal defense mechanisms (Fig. 4).
2. A ‘silent’  $\text{Ca}^{2+}$  response 10–60 min after challenge may reflect a transition period from a basal PAMP-triggered response to the sustained *R*-gene-dependent calcium increase, similarly to what was proposed by Grant et al. (2000).

**Table 1** Net  $\text{K}^{+}$  flux values measured from leaf mesophyll samples following 24 h of inoculation with *P. syringae* pv *syringae* 61

	Control	<i>P. syringae</i> -inoculated
Light	$-14.9 \pm 8.6$	$-7.46 \pm 4.46$
Dark	$-1.03 \pm 0.54$	$2.52 \pm 4.32$

Mean  $\pm$  SE ( $n = 4-8$ ).

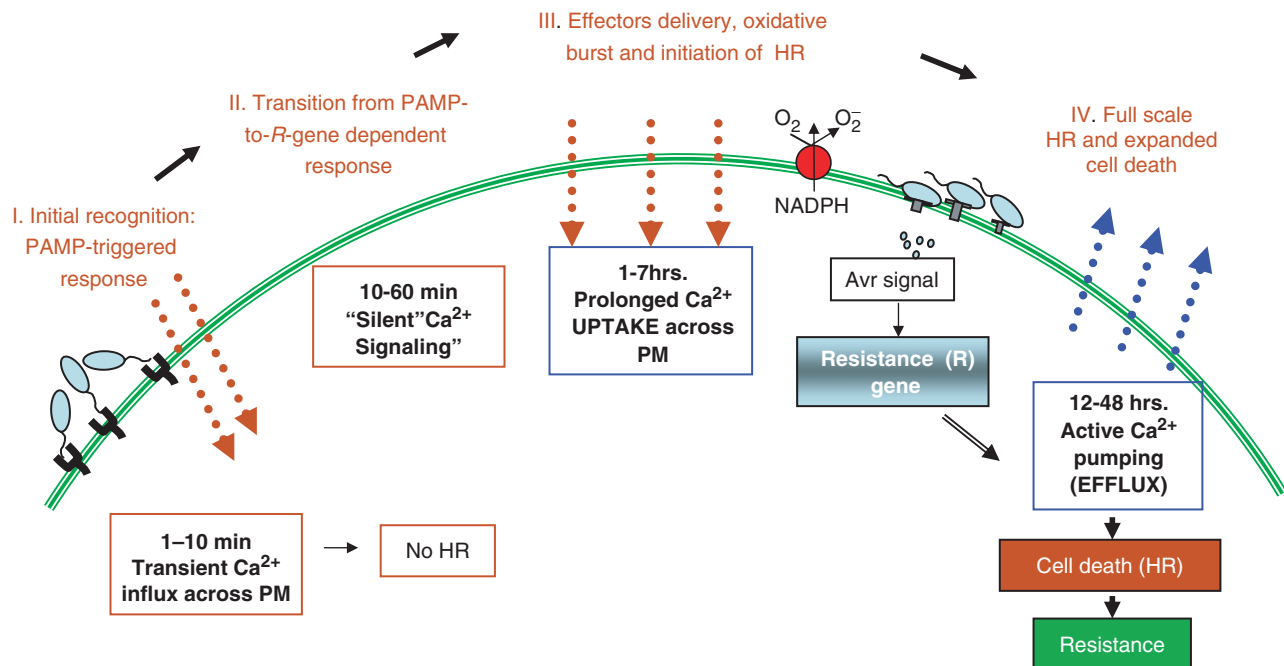


**Fig. 4** The proposed timing of calcium ion fluxes in mediation of plant defense responses. PAMP, pathogen-associated molecular patterns; HR, hypersensitive response; PM, plasma membrane; NADPH, nicotinamide adenine dinucleotide phosphate oxidase-mediated production of reactive oxygen species (ROS) in the form of  $\text{O}_2^-$ .



3. Prolonged  $\text{Ca}^{2+}$  uptake, which continues to occur 1–7 h after the challenge, reflects the pathogen's successfully overcoming the initial PAMP-triggered defense reaction (Jones and Dangle 2006). Sustained increases in  $\text{Ca}^{2+}$  at this stage are necessary for generation of reactive oxygen species (ROS), the oxidative burst and induction of the HR (Atkinson et al. 1990, Grant et al. 2000).
4. After the HR transduction pathway has been initiated with the help of  $\text{Ca}^{2+}$  uptake, calcium levels sharply decline to what we believe corresponds to the last HR phase—an expanded cell death (Fig. 4). Consequently, downstream  $\text{Ca}^{2+}$  efflux rather than uptake could participate in and/or be required for cell death and tissue collapse during the HR. Similar observations, although indirectly, suggested the role of calcium lowering during the tobacco mosaic virus-induced HR in tobacco plants containing the *N* resistance gene (Mittler et al. 1999). Complete tissue collapse and restriction of pathogen movement corresponds to a fourth and last phase of HR. Calcium fluxes in or around the HR site return to background levels and the defense cycle is now complete (Fig. 4).

The proposed sequence of calcium defense-related signaling represents a novel view for the role of  $\text{Ca}^{2+}$  in plant response to microbial challenge. Particularly, our data suggest that calcium acts not only as an important second messenger in the activation of resistance responses (Grant et al. 2000, Balagué et al. 2003, Lecourieux et al. 2006) but possibly also as a downstream mediator of later cell death acceleration, inhibition of the spread of invading pathogens and completion of the defense reaction. Accordingly, we suggest that the existing model of HR should be amended to include a PM  $\text{Ca}^{2+}$  pump as an important component of the HR to pathogens in plants.

## Materials and Methods

### Bacterial strains, media and growth conditions

*Pseudomonas syringae* pv *syringae* 61 and *P. syringae* pv *tabaci* were obtained from N. Mock and C. J. Baker, USDA/ARS/PSI/MPPL. Bacteria were grown overnight in 5 ml of King's B (KB) medium (King et al. 1954). For *P. syringae* pv *syringae* 61, the medium was supplemented with  $20 \mu\text{g ml}^{-1}$  of nalidixic acid at  $30^\circ\text{C}$ . Inoculum for infiltration assays was obtained by harvesting bacteria for 10 min at 4,000 r.p.m. (relative centrifugal force  $2.5\times g$ ) in an Eppendorf bench-top centrifuge model 5702 R and suspending in 5 ml of deionized water. After this washing step was repeated twice, the bacterial culture was adjusted to appropriate cell densities of  $\text{OD}_{600}$  0.2 ( $\sim 2\times 10^8$  cells  $\text{ml}^{-1}$ ).

### Plant material and inoculation

*Nicotiana benthamiana* plants were grown in MPPL's containment greenhouse facility in Beltsville, MD, with supplementary lamp illumination and a photoperiod of 16 h. Fully expanded, similar sized and aged leaves of 1-month-old plants were used for the infiltration of  $50 \mu\text{l}$  of bacteria through a small dissecting-needle wound by pressing the blunt end of a syringe without the needle against the leaf surface while supporting the leaf with a finger (Huang et al. 1988). Control plants were mock infiltrated with distilled water.

### Non-invasive ion flux measurements

Net  $\text{Ca}^{2+}$  and  $\text{K}^+$  fluxes were measured non-invasively using the MIFE technique. All details on microelectrodes fabrication and calibration are given elsewhere (Shabala 2000). Three types of experiments were conducted. In long-term treatments, *N. benthamiana* leaves were excised at some specific time after inoculation. The abaxial epidermis was gently removed at the sites of bacterial infiltration, and mesophyll segments of about  $3\times 5$  mm were cut and left floating (peeled side down) on a surface of measuring solution ( $0.1 \text{ mM CaCl}_2 + 0.2 \text{ mM KCl}$ ; pH 6 unbuffered) for at least 3 h to avoid potential wounding effects. Prior to measurement, mesophyll segments were immobilized in a Perspex holder and placed in a measuring chamber. For short-term bacterial treatments (1–3 h), healthy leaves were excised and mesophyll segments prepared as described above. Leaf segments were then placed peeled side down on the  $50\text{--}100 \mu\text{l}$  of bacterial inoculum and incubated in a closed 6 cm Petri dish. Net  $\text{Ca}^{2+}$  or  $\text{K}^+$  fluxes were measured at specific time intervals after incubation. Finally, in transient experiments, net  $\text{Ca}^{2+}$  ion fluxes were first measured from healthy mesophyll segments for 5–10 min, after which bacterial inoculum stock was added directly to the measuring chamber, making the final concentration  $\sim 4\times 10^7$  cells  $\text{ml}^{-1}$ .

An ion-selective microelectrode was positioned  $50 \mu\text{m}$  above the leaf surface. During the measurements, electrodes were moved back and forth in a square-wave manner by a computerized stepper motor between two positions ( $50$  and  $120 \mu\text{m}$  above the leaf surface) with  $0.125 \text{ Hz}$  frequency. Net ion fluxes were calculated from measured differences in the electrochemical potential between these two positions for each ion, as described earlier (Shabala et al. 1997). Most measurements were conducted under dim ( $20 \mu\text{mol s}^{-1} \text{ m}^{-2}$ ) and bright ( $2,500 \mu\text{mol s}^{-1} \text{ m}^{-2}$ ) light regimes using an inverted microscope model RTC-6 (Radical Instruments, India).

### Pharmacology

Prior to measurement, leaf segments were pre-treated for 1 h with a range of known  $\text{Ca}^{2+}$ -permeable channel blockers or  $\text{Ca}^{2+}$ -ATPase metabolic inhibitors. These included: (i) gadolinium chloride ( $\text{Gd}^{3+}$ ;  $50 \mu\text{M}$ ); (ii) lanthanum chloride ( $\text{La}^{3+}$ ,  $1 \text{ mM}$ ); (iii) cesium chloride ( $\text{Cs}^+$ ,  $1 \text{ mM}$ ); and (iv) CPA ( $50 \mu\text{M}$ ). All chemicals were purchased from Sigma.

### Statistical analysis

The statistical significance of mean values was determined using the standard Student's *t*-test at the  $P < 0.05$  level.

## Funding

United States Department of Agriculture/Agricultural Research Service, to L.G.N.; Australian Research Council

Discovery; Tasmanian Institute of Agricultural Research, to S.S. and L.S.

### Acknowledgments

We are grateful to C. J. Baker and N. Mock of the Molecular Plant Pathology Laboratory, USDA/ARS, for *P. syringae* strains; J. C. Dickens of the Insect Behavior Laboratory and J. Bunce of the Crop Systems and Global Change Laboratory, USDA/ARS for sharing their equipment. We would also like to thank the anonymous reviewers for their time and valuable comments.

### References

- Atkinson, M.M., Keppler, L.D., Orlandi, E.W., Baker, C.J. and Mischke, C.F. (1990) Involvement of plasma membrane calcium influx in bacterial induction of the  $K^+/H^+$  and hypersensitive responses in tobacco. *Plant Physiol.* 92: 215–221.
- Balagué, C., Lin, B., Alcon, C., Flottes, G., Malmström, S., Köhler, C., Neuhaus, G., Pelletier, G., Gaymard, F. and Roby, D. (2003) HLM1, an essential signaling component in the hypersensitive response, is a member of the cyclic nucleotide-gated channel ion channel family. *Plant Cell* 15: 365–379.
- Elzenga, J.T.M., Prins, H.B.A. and Van Volkenburgh, E. (1995) Light-induced membrane potential changes of epidermal and mesophyll cells in growing leaves of *Pisum sativum*. *Planta* 197: 127–134.
- Flor, H.H. (1971) Current status of gene-for-gene concept. *Annu. Rev. Phytopathol.* 9: 275–296.
- Gilroy, S., Bethke, P.C. and Jones, R.L. (1993) Calcium homeostasis in plants. *J. Cell Sci.* 106: 453–462.
- Gómez-Gómez, L. and Boller, T. (2002) Flagellin perception: a paradigm for innate immunity. *Trends Plant Sci.* 7: 251–256.
- Grant, M., Brown, I., Adams, S., Knight, M., Ainslie, A. and Mansfield, J. (2000) The RPM1 plant disease resistance gene facilitates a rapid and sustained increase in cytosolic calcium that is necessary for the oxidative burst and hypersensitive cell death. *Plant J.* 23: 441–450.
- Hann, D.R. and Rathjen, J.P. (2007) Early events in the pathogenicity of *Pseudomonas syringae* on *Nicotiana benthamiana*. *Plant J.* 49: 607–618.
- Heath, M.C. (2000) Hypersensitive response-related death. *Plant Mol. Biol.* 44: 321–334.
- Huang, H.C., Schuurink, R., Denny, T.P., Atkinson, M.M., Baker, C.J., Yucel, I., Hutcheson, S.W. and Collmer, A. (1988) Molecular cloning of a *Pseudomonas syringae* pv. *syringae* gene cluster that enables *Pseudomonas fluorescens* to elicit the hypersensitive response in tobacco plants. *J. Bacteriol.* 170: 4748–4756.
- Jabs, T., Tschöpe, M., Colling, C., Hahlbrock, K. and Scheel, D. (1997) Elicitor-stimulated ion fluxes and  $O_2^-$  from the oxidative burst are essential components in triggering defense gene activation and phytoalexin synthesis in parsley. *Proc. Natl Acad. Sci. USA* 94: 4800–4805.
- Jones, J.D. and Dangle, J.L. (2006) The plant immune system. *Nature* 444: 323–329.
- King, E.O., Ward, M.K. and Raney, D.E. (1954) Two simple media for the demonstration of pyocyanin and fluorescein. *J. Lab. Clin. Med.* 22: 301–307.
- Lam, E., Kato, N. and Lawton, M. (2001) Programmed cell death, mitochondria and the plant hypersensitive response. *Nature* 411: 848–853.
- Lecourieux, D., Ranjeva, R. and Pugin, A. (2006) Calcium in plant defence-signalling pathways. *New Phytol.* 171: 249–69.
- Levine, A., Pennell, R.I., Alvarez, M.E., Palmer, R. and Lamb, C. (1996) Calcium-mediated apoptosis in a plant hypersensitive disease resistance response. *Curr. Biol.* 6: 427–437.
- Mittler, R., Lam, E., Shulaev, V. and Cohen, M. (1999) Signals controlling the expression of cytosolic ascorbate peroxidase during pathogen-induced programmed cell death in tobacco. *Plant Mol. Biol.* 39: 1025–1035.
- Pike, S.M., Zhang, X.C. and Gassmann, W. (2005) Electrophysiological characterization of the *Arabidopsis* avrRpt2-specific hypersensitive response in the absence of other bacterial signals. *Plant Physiol.* 138: 1009–1017.
- Quiquampoix, H., Ratcliffe, R.G., Ratkovic, S. and Vucinic, Z. (1990) A  $^1H$  and  $^{31}P$  NMR investigation of gadolinium uptake in maize roots. *J. Inorg. Biochem.* 38: 265–275.
- Shabala, L., Ross, T., McMeekin, T. and Shabala, S. (2006) Non-invasive microelectrode ion flux measurements to study adaptive responses of microorganisms to the environment. *FEMS Microbiol. Rev.* 30: 472–486.
- Shabala, S. (2000) Ionic and osmotic components of salt stress specifically modulate net ion fluxes from bean leaf mesophyll. *Plant Cell Environ.* 23: 825–837.
- Shabala, S. and Newman, I.A. (2000) Salinity effects on the activity of plasma membrane  $H^+$  and  $Ca^{2+}$  transporters in bean leaf mesophyll: masking role of the cell wall. *Ann. Bot.* 85: 681–686.
- Shabala, S., Newman, I.A. and Morris, J. (1997) Oscillations in  $H^+$  and  $Ca^{2+}$  ion fluxes around the elongation region of corn roots and effects of external pH. *Plant Physiol.* 113: 111–118.
- Van Volkenburgh, E. (1999) Leaf expansion—an integrating plant behavior. *Plant Cell Environ.* 22: 1463–1473.
- Zivanovic, D.B., Cuin, T.A. and Shabala, S. (2007) Spectral and dose dependence of light-induced ion flux responses from maize leaves and their involvement in leaf expansion growth. *Plant Cell Physiol.* 48: 598–605.

(Received October 11, 2007; Accepted November 19, 2007)